20th Australasian Fluid Mechanics Conference
Perth, Australia
5-8 December 2016

Preliminary Development of High Enthalpy Conditions for the X3 Expansion Tube

A. Andrianatos[1], **D. Gildfind**[1] **and R. Morgan**[1]

[1]Centre for Hypersonics
School of Mechanical and Mining Engineering
University of Queensland, Queensland 4072, Australia

Abstract

The University of Queensland (UQ) operates two free piston [1] driven expansion tubes - X2, and the larger X3 - for conducting simulations of atmospheric entry. Recently, high enthalpy experiments have only been performed in X2 but there is interest to develop the capability for high enthalpy experimentation in X3 as it's size allows for experimentation with larger scale models. To achieve these conditions, a new light weight piston and reservoir extension have been commissioned. This paper presents a preliminary investigation into the development of new operating conditions for X3 using the recent upgrades.

Introduction

The conditions experienced during atmospheric entry are amongst the harshest a vehicle will experience. At superorbital velocities a vehicle will enter Earth's atmospehere in excess of $10\mathrm{km\,s^{-1}}$ and temperatures behind the shock layer in front of the vehicle are on the order of 10,000K. Heat transfer to the surface of the vehicle by radiation becomes a significant mode of heat transfer [2]. While convective heat transfer to the vehicle can be estimated reasonably well, the nonequilibrium radiation phenomena are still not well understood [3] which leads to large factors of safety in the design of thermal protection systems.

The size limitation of experimental facilities typically require that small subscale models of flight vehicles are used. When scaling models for experimental use, assuming flight enthalpy is matched, binary scaling can be used to ensure similarity between the experimental and flight condition [4]. This scales as the density length product between the two conditions (ρL) which conserves Reynolds number and viscous effects, and matches binary chemical reactions in the flow field. The similarity starts to break down when radiation is considered as the mass flux into the shock layer scales with area (ρL^2), and the heat lost via radiation scales with volume (ρL^3) which results in insufficient heat removal via radiation in the scaled experiment. True similarity between experiment and flight is lost and the significance depends on the strength of the coupling between the radiation and the flow properties. If the flow is strongly coupled, then changes to the flow field will occur and the facility will not produce direct simulation of the flight [4].

High enthalpy experiments have been conducted in [5] of a 1:5 subscale Hayabusa re-entry capsule model. The experiments were conducted to provide a comparison between flight and numerical data. High enthalpy conditions used in [5] will be replicated in X3 with a same scale model as X2, which is the primary focus of this paper. X2's operating condition will be scaled in the future to test larger scale models in X3: up to $1:2$ scale models with the current hardware to investigate how the flowfield is affected by scaling.

X3 Expansion Tube

The X3 expansion tube consists of (upstream to downstream): reservoir, piston, driver tube, primary diaphragm, secondary driver tube (optional), secondary diaphragm (optional), shock tube, tertiary diaphragm, and acceleration tube. The reservoir is filled with high pressure air which accelerates a piston along the driver tube. The piston compresses the driver gas, typically a helium argon mixture, until the primary diaphragm ruptures. The high pressure driver gas drives a shock into the secondary driver compressing and heating the secondary driver gas. After the secondary diaphragm ruptures, the resulting shock into the shock tube compresses and heats the test gas. Unlike a conventional shock tunnel, the test gas unsteadily expands into the acceleration tube rather than stagnates before a nozzle throat. Unsteadily expanding the test gas increases the total pressure and enthalpy achieveable because no gas stagnation structure is required and chemical reactions in the high temperature test gas is avoided. At the end of the acceleration tube the test gas undergoes a steady expansion through a nozzle into the test section.

Piston and Reservoir Upgrades

A new lightweight piston has been developed [6], which weighs 100.8kg compared to the previous 200kg piston. Additionally an extension to the reservoir has been installed to allow for larger volumes of high pressure gas behind the piston. This effectively increases the operating capacity of the driver as less reservoir pressure will be required to replicate a driver condition. Using less pressure allows for higher pressures to drive the piston faster then previously achieveable. Figure 1 and figure 2 show the lightweight piston and reservoir extension.

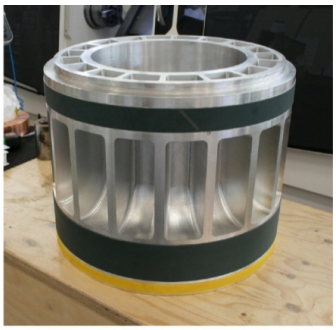

Figure 1: New lightweight piston, taken from [6]

The purpose of both of these upgrades is to increase the performance and range of operating conditions of the driver. To increase the performance of the driver, the facility can be operated with a higher compression ratio of driver gas, which can be achieved by starting with a lower driver pressure or by increasing the diaphragm rupture pressure; or the helium concentration of the driver gas can be increased (i.e. an increase in sound speed).

When using a high sound speed driver, the driver gas vents more rapidly after diaphragm rupture and "tuning" the piston is a method to sustain driver pressure. The design of the free-piston driver makes use of a "tuned" condition when firing the piston [1] [7]."Tuning" involves running the piston with a high velocity when the diaphragm ruptures. Unlike a constant volume driver, the motion of the piston counteracts the driver gas venting into

Figure 2: Reservoir extension.

the tube and a near to constant driver pressure is obtained, for potentially much longer durations.

The driver operating range is limited by the trajectory of the piston. It is necessary to avoid the piston striking the end of the driver tube with a considerable velocity to prevent damage to the tube. This is achieved by designing piston trajectories with an inflection point, and limiting the extent that the pressure can continue to increase after diaphragm rupture (overdrive)[8], as done with X2's lightweight piston [7]. The inflection point - where the piston has zero velocity and zero acceleration - is a location where the piston can be caught without risking facility or piston damage.

Analytical Driver Performance

Analytical piston trajectories were calculated using a method outlined by Hornung [9]. While Hornung makes assumptions regarding the behavior of the gas behing and in front of the piston, there is still useful information that can be acquired from the model. The assumption that the reservoir is an infinitely long tube to simplify the gas process behind the piston results in reservoir pressures that do not represent reality. Hornung also assumes that the driver gas pressure increase is spatially uniform, and ignores wave processes, since the piston velocity is very subsonic compared to the sound speed of helium. The combination of these assumptions result in useful data after the diaphragm has ruptured, when the driver pressure is high and the deceleration of the piston is mainly due to the driver gas. Useful information about the piston trajectory and driver gas pressure can be obtained after diaphragm rupture near the end of the piston's stroke.

The existence of an inflection point is imposed on the trajectory and the pressure after diaphragm rupture is restricted to a maximum of $\pm 10\%$ of the rupture pressure before the driver pressure is considered outside acceptable limits [8]. This results in a series of potential piston trajectories that overdrive the driver gas pressure up to 10% over rupture pressure.

Analytical trajectories were calculated for a range of overdrive values. Figure 3 shows the required driver gas fill pressure to satisfy a "tuned" piston trajectory for various amounts of overdrive for the 2mm diaphragm (17.5MPa). For a pure argon driver, 0% helium, the required driver fill pressure for all conditions fall between $45-55$kPa. The fill pressure rapidly increases up to $300-600$kPa as higher concentrations of helium are used.

To gauge the performance of each driver condition the shock speed produced into a shock tube of 13.5kPa of air was also calculated. This pressure is chosen as it will be used to develop an X2 crossover condition in X3, and depending on the performance of X3 will give a relative perfomance comparison to X2. Shock speeds have been calculated using PITOT [10], an

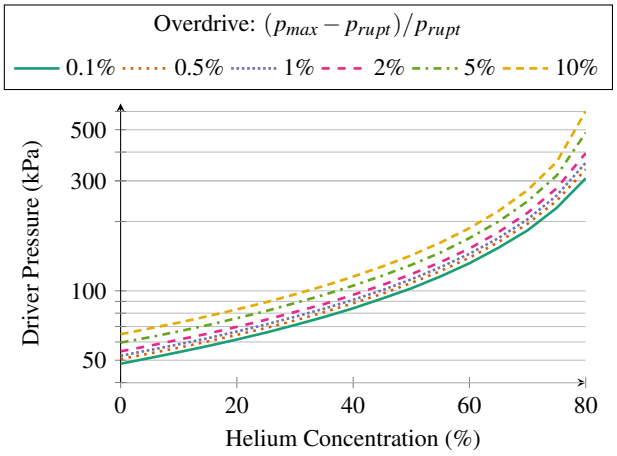

Figure 3: Required driver pressure for different helium concentrations and different levels of overdrive. p_{max} is the maximum pressure obtained and p_{rupt} is the rupture pressure.

analytical expansion tube solver which utilises equilibrium gas models which account for high temperature effects. Figure 4 contains the shock speeds produced using the driver fressure and compositions in figure 3. Higher concentrations of helium require a large increase in driver pressure but only increases the shock speed by 20%. Increasing the helium concentration of the driver gas also requires a fill pressure increase (figure 3), the consequence of this is that the driver gas is not compressed to as high a temperature and this conteracts the effect of adding more helium.

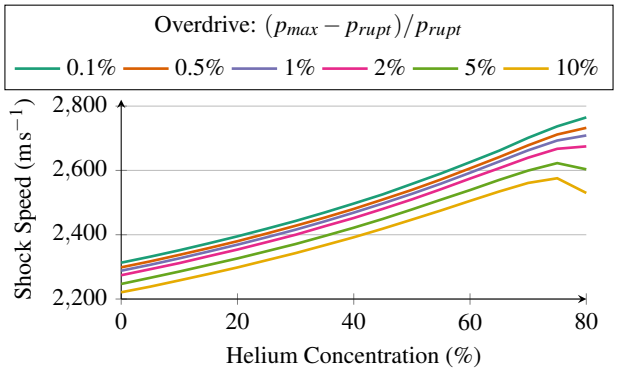

Figure 4: Shock speeds into shock tube of 13.5kPa air.

The helium percentage can also be increased using orifice plates [11] at the exit of the driver tube. The presence of an orifice plate restricts the flow of driver gas into the tube and higher concentrations of helium can be used without requiring such high driver fill pressures. If a working condition with 100% argon is known, which has been selected since is requires the lowest fill pressure; a similar condition with a higher concentration of helium can be used with an appropriately sized orifice plate. The diameter of the orifice plate can be calculated using:

$$\frac{D^*}{D_d} = \sqrt{\frac{A^*}{A_d}} = \left(\frac{R_{D,1}}{R_{D,2}}\right)^{0.25} \tag{1}$$

In equation (1), D_d and A_d are the diameter and area of the shock tube, which corresponds to the 100% argon condition. D^* and A^* are the diameter and area of the orifice plate; for a high helium concentration. $R_{D,1}$ is the gas constant for argon and $R_{D,2}$ is the gas constant for the helium argon mixture. Equation (1) does not necessarily need to be used from a 100% base, but can be used to scale an orifice plate between any two helium concentrations.

several orifice plate diameters have been considered for various helium concentrations are shown in table 1.

100% Argon:0% Helium	200.0mm
40% Argon:60% Helium	164.7mm
20% Argon:80% Helium	145.5mm
0% Argon:100% Helium	112.5mm

Table 1: Orifice diameters for different helium concentrations.

When accounting for the orifice and lower fill pressures for high helium concentrations, the shock speeds in figure 5 are achieved. In general, using an orifice plate as a means to increase helium concentration provides a greater increase in shock speed than simply increasing helium concentration as in figure 3 and figure 4 when accounting for the limitations imposed on the driver. X3 can be operated with three diaphragm thicknesses; 2mm, 3mm, and mm which rutpure at 17.5MPa, 26.25MPa, and 35MPa respectively. Figure 5 only includes conditions for the 2mm and 4mm diaphragms. Similar analysis for the 3mm diaphragm results in shock speeds on the order of 4200m s^{-1}.

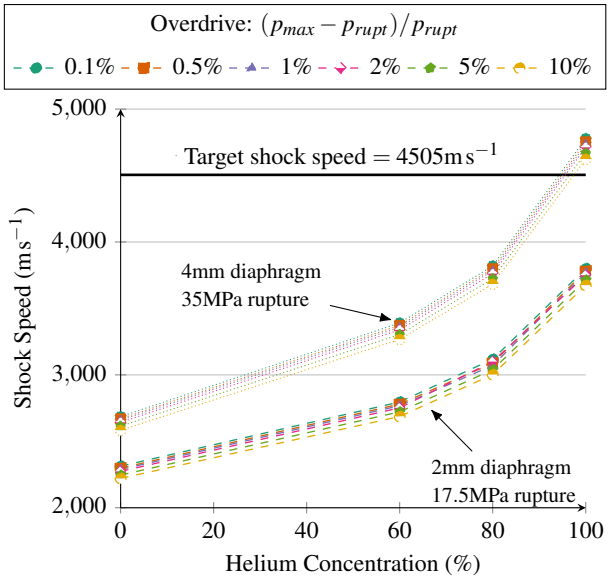

Figure 5: Shock speeds in 13.5kPa air with orifice plate. The dashed lines correspond to the 2mm diaphragm and the dotted lines correspond to the 2mm diaphragm. The black solid line is the target shock speed for an X2 crossover condition.

X2 crossover

As radiation experiments will be conducted using an X2 condition [5] as a basis, a crossover condition that results in the same test flow properties needs to be developed. Regardless of whether a secondary driver is used, the shock tube and acceleration tube fill pressures are the same and are given in table 2.

Shock tube fill pressure	13.5kPa
Shock tube shock speed	4505m s^{-1}
Acceleration tube fill pressure	17Pa
Acceleration tube shock speed	10145m s^{-1}

Table 2: X2 fill pressure and nominal shock speeds

Since X2 and X3 are functionally similar facilities, and the nozzle on each facility is a scaled version of the other, the condition in table 2 can be reproduced in X3 if the fill pressures and shock speeds are matched. The difference between the two facilities is the driver so a condition for X3's driver must be found that produces the same shock speeds. The target shock speed can be exceeded using a 4mm diaphragm although this is an ideal estimate and does not account for losses in the driver.

X3 can also be operated with a secondary driver. Using a secondary driver adds complexity to the condition building procedure, but it allows for faster shock speeds to be generated in the shock tube when the shock processed secondary driver gas has a faster shock speed than the expanded driver gas [12]. Commissioning tests with the new piston and reservoir were completed with a 53kPa argon driver pressure. As experimental information is already known for this condition it will be used when analysing the use of a secondary driver.

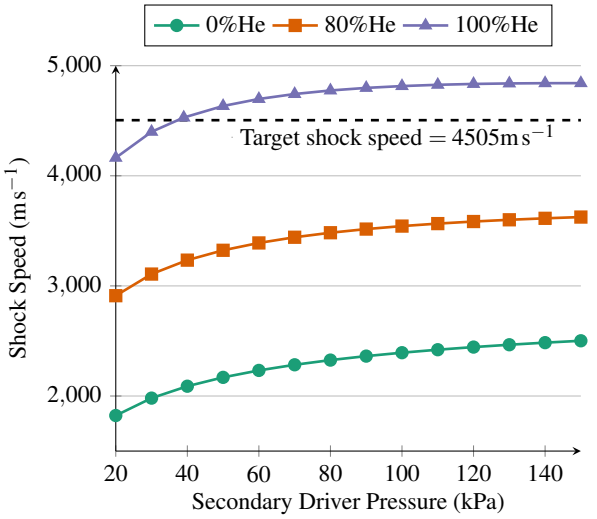

Figure 6: Shock speeds using 53kPa driver with different helium concentrations. All curves use a 17.5MPa rupture pressure and the overdrive is approximately 1%.

Figure 6 shows that using a secondary driver enables the facility to achieve the desired shock speed with a 2mm driver, which was not obtainable in figure 5. While increasing the secondary driver pressure does increase the shock speed, this is an effect of diminishing returns, and changing the driver composition has a more significant effect on the shock speed.

	No secondary driver	Secondary Driver
Diaphragm thickness	4mm	2mm
Driver pressure	45 – 58kPa	53kPa
Driver composition	100% He	100% He
Secondary driver pressure	N/A	39kPa

Table 3: Driver condition summary for working conditions with and without a secondary driver. Both driver conditions are achieved using an orifice plate.

A summary of working conditions with and without a secondary driver is shown in table 3. One potential limitation to achieving the "no secondary driver" condition may be the reservoir fill pressure, but until further numerical simulations and experimental investigations are completed the final driver operation condition cannot be confirmed.

Numerical Simulations

This section outline numerical simulations of X3's driver that have been completed using L1d, a 1-D Lagrangian code for the simulation of transient facilities [13] and also accounts for piston motion. L1d simulations tailored with experimental data can be used to model the facility. L1d models the facility in one dimension; whereas X3's driver and reservoir configuration are very three dimensional. If the volume and length of each section is approximately correct, loss factors can be added to L1d to

account for any pressure and other loss mechanisms due to three dimensional effects.

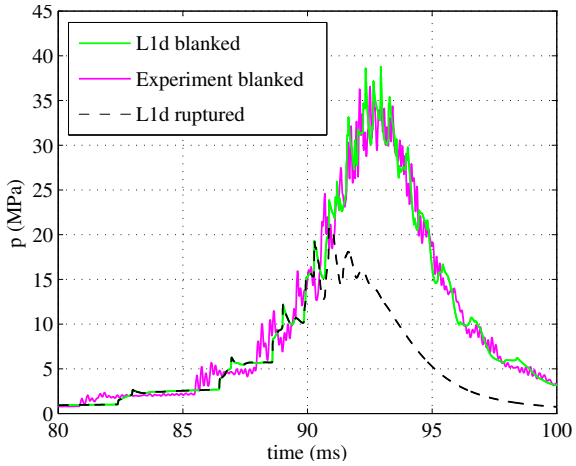

Figure 7: Comparison of blanked off shot with L1d simulation of blanked off shot and 17.5MPa rupturing diaphragm[6].

During commissioning of the piston and reservoir, blanked off shots (using a non-rupturing steel plate rather than the normal rupturing steel diaphragm) were performed and the pressure data in the driver has been used to tailor the L1d model of the driver and reservoir. The driver pressure recorded during the blanked off shot contains the forwards and backwards stroke of the piston, as the diaphragm doesn't rupture. Additionally, shots using a 53kPa driver and no reservoir extension were previously performed in [6]. Figure 7 shows the measured pressure trace from [6] and compares it to L1d simulations.

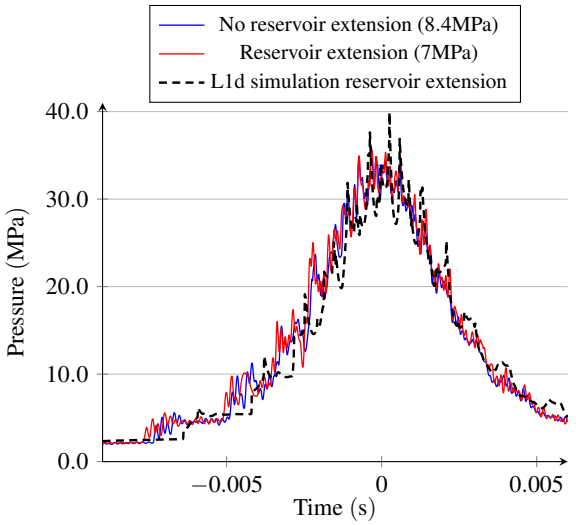

Figure 8: Comparison of experimental blanked off shots with and without the reservoir with L1d using the reservoir.

The blanked off shot in figure 7 was used as a reference for gauging the performance of the reservoir extension. It was found that the pressure trace could be replicated using a 7MPa reservoir pressure compared to an 8.4MPa reservoir pressure when not using the extension. Figure 8 shows the comparison between the two experimental shots and an updated L1d simulation using the new reservoir geometry. It should be noted that the wave processes are matched well between the two experimental shots (red and black), but not well matched with the L1d. This has been put down to a difference in piston velocity at the beginning of the piston stroke. More importantly, the general shape of the area curve, and features after peak pressure are quite consistent, so it can be said that the L1d simulation accurately represents the facility around the time of diaphragm rupture. Simulations with the aim of matching the wave processes on the forwards stroke has not been completed.

Conclusions

The primary objective of this study is to investigate how radiating shock layers scale with model size using the X3 facility. X3 will be used because it is a larger facility and will allow for larger scale models to be tested compared to those done previously in X2. To achieve these conditions a new light weight piston and reservoir extension have been designed. An X2 crossover condition can be achieved in X3 with the use of the light weight piston and reservoir extension; either using a secondary driver or without one. Further experimental work is still required to validate analytical and numerical models, particulary relating to diaphragm rupture. Once a working condition for X3's driver is developed further work can be done in developing the final condition for high enthalpy experiments in X3.

Acknowledgements

The authors wish to thank: Mr F. De Beurs and Mr N. Duncan for technical support; The Australian Research Council for support and funding; The Queensland Smart State Research Facilities Fund 2005 for support and funding and The Australian Space Research Program.

References

[1] R.J. Stalker. "A study of the free-piston shock tunnel." *AIAA Journal* 5.12 (1967).

[2] J.D. Anderson JR. "An engineering survey of radiating shock layers." *AIAA Journal* 7.9 (Sept. 1969).

[3] S.P. Sharma and E.E. Whiting. "Modeling of nonequilibrium radiation phenomena - An assessment". *Journal of Thermophysics and Heat Transfer* 10.3 (July 1996).

[4] RG Morgan et al. "Impulse facilities for the simulation of hypersonic radiating flows". *38th Fluid Dynamics Conference and Exhibit, Seattle, Washington*. 2008.

[5] Elise J Fahy et al. "Expansion Tube and Computational Fluid Dynamics Studies of Superorbital Earth Re-entry". *46th AIAA Thermophysics Conference* (2016).

[6] D.E. Gildfind et al. "Design and commissioning of a new lightweight piston for the X3 Expansion Tube". *29th International Symposium on Shock Waves*. Springer. 2014.

[7] D.E. Gildfind et al. "Free-piston driver optimisation for simulation of high Mach number scramjet flow conditions". *Shock Waves* 21 (2011).

[8] K. Itoh et al. "Improvement of a free piston driver for a high-enthalpy shock tunnel". *Shock Waves* 8.4 (1998).

[9] H.G. Hornung. "The piston motion in a free-piston driver for shock tubes and tunnels". *GALCIT Report FM* (1988).

[10] C.M. James et al. "Designing and Simulating High Enthalpy Expansion Tube Conditions". *2013 Asia-Pacific International Symposium on Aerospace Technology*. Takamatsu, Japan, 2013.

[11] D.E Gildfind et al. "Free-piston driver performance characterisation using experimental shock speeds through helium". *Shock Waves* 25 (2 2015).

[12] R.G. Morgan and R.J. Stalker. "Double diaphragm driven free piston expansion tube". *Shock waves; Proceedings of the 18th International Symposium*. 1992.

[13] P.A. Jacobs. *L1d: A computer program for the simulation of transient-flow facilities. Report 1/99*. Australia: University of Queensland, 1999.